2019

Bacteria-Resistant, Transparent, Free-standing Films Prepared from Complex Coacervates

Irene S. Kurtz
University of Massachusetts Amherst

Shuo Sui
University of Massachusetts Amherst

Mengfei Huang
University of Massachusetts Amherst

Jessica D. Schiffman
University of Massachusetts Amherst

Sarah L. Perry
University of Massachusetts Amherst

Recommended Citation
Kurtz, Irene S.; Sui, Shuo; Huang, Mengfei; Schiffman, Jessica D.; and Perry, Sarah L., "Bacteria-Resistant, Transparent, Free-standing Films Prepared from Complex Coacervates" (2019). *ACS Applied Bio Materials*. 870.
https://doi.org/10.1021/acsabm.9b00502

Bacteria-Resistant, Transparent, Free-standing Films Prepared from Complex Coacervates

Irene S. Kurtz†, Shuo Sui†, Xi Hao†, Mengfei Huang, Sarah L. Perry*, and Jessica D. Schiffman*

Department of Chemical Engineering, Institute of Applied Life Sciences, University of Massachusetts Amherst, Amherst, MA 01003

†These authors contributed equally.

* Corresponding authors: Jessica D. Schiffman, Email: schiffman@ecs.umass.edu; Sarah L. Perry, Email: perrys@engin.umass.edu

ABSTRACT

We report the fabrication, properties, and bacteria-resistance of polyelectrolyte complex (PEC) coatings and free-standing films. Poly(4-styrenesulfonic acid), poly(diallyldimethylammonium chloride), and salt were spin-coated into PEC films. After thermal annealing in a humid environment, highly transparent, mechanically strong, and chemically robust films were formed. Notably, we demonstrate that PEC coatings significantly reduce the attachment of *Escherichia coli* K12 without killing the microorganisms. We suggest that forming bacteria-resistant surface coatings from commercially available polymers holds the potential for use across a wide range of applications, including high-touch surfaces in medical settings.

KEYWORDS: Antifouling, Complex coacervation, *Escherichia coli,* Polyelectrolyte, Spin-coating

INTRODUCTION

Inanimate surfaces in intensive care units (ICUs), such as bedrails, medical charts, and monitors, act as reservoirs for bacteria and cross-contamination, often leading to patient colonization and infections.[1] Notably, approximately 60% of bacterial infections in ICUs are due to cross-transmission, necessitating effective and affordable means of preventing the initial attachment of bacteria.[1] Typically, antifouling coatings feature hydrophilic polymers, such as poly(ethylene glycol) (PEG) or polymer zwitterions,[2–4] which prevent bacterial adhesion by attracting water molecules to the surface, creating a hydration barrier to bacterial attachment.[5,6] In particular for polymer zwitterion coatings, the close proximity of oppositely charged groups facilitates the formation of ionic bonds with water molecules, creating an aqueous layer that prevents the adsorption of organic and biological materials.[5–8] While PEG and polymer zwitterion-based coatings are highly effective at reducing bacterial adhesion by at least 85%,[4,9–14] they often involve complex synthesis[15–17] and substrate specific methods for surface immobilization.[9,18–21] PEG is used extensively in commercial applications,[22–25] but it can degrade in biological conditions[26–30] and PEG antibodies have been reported. Thus, developing alternative means of addressing biological fouling is needed.[31–33]

Polyelectrolyte complexes (PECs) form through the electrostatic and entropic interactions between oppositely-charged polymers that lead to the release of bound counterions and the restructuring of the surrounding aqueous phase.[34–36] The resulting complexes can undergo liquid-liquid phase separation (*i.e.*, complex coacervation) or liquid-solid phase separation depending on

the identity and length of the polymers, and the solution conditions, including the ionic strength and pH value.[34,37,38] While PECs have been used in a range of applications including drug delivery, advanced adhesives, and food science,[34,39,40] most of this work has been focused on liquid complex coacervates. The utility of solid PEC complexes has historically been limited as the strong electrostatic interactions that drive complexation prohibits traditional thermal and/or solvent processing methods. However, recent work has demonstrated that salt can be used to plasticize PECs to enable processing.[41–48] To date, PECs have been extruded into single fibers,[44,49] electrospun into fiber meshes,[41,42] processed into free-standing microchambers,[46] spin-coated into films,[43] cast into films[45] and 3D-printed into material forms.[50,51]

Because PECs consist of oppositely-charged polymers, we hypothesized that their positive and negative charges might mirror the functionality of polymer zwitterions, creating a barrier against bacterial attachment.[3,5,6] Notably, layer-by-layer films show changes in wetting, indicating a possible hydration barrier.[52–54] Previously, researchers have studied the antibacterial (killing) properties of silver nanoparticle-embedded polyelectrolyte layer-by-layer films,[55] the flux recovery of layer-by-layer coated membranes,[56] as well as their antifouling performance against diatom cells and barnacles.[56,57] Another study described how ultracentrifugated compact PECs from chitosan and alginate resisted the adhesion of *Staphylococcus aureus*.[58] While this result is encouraging, there is a benefit to developing alternative processing strategies that are less energy intensive and can be performed at scale to enable the use of PECs as antifouling coatings.

Here, we report the fabrication of transparent, resilient, free-standing PEC films via spin-coating and have investigated their application as bacteria-resistant coatings. PECs were formed using two low-cost, commercially-available commodity polyelectrolytes, poly(4-styrenesulfonic acid) and poly(diallyldimethylammonium chloride) with potassium bromide (KBr) salt. Spin-

coated films were prepared using various post-processing techniques and their transparency, ultimate tensile strength, thickness, and resistance to the attachment of *Escherichia coli* K12 MG1655 was determined. Our strategy for the aqueous processing of low-cost polymers into antifouling coatings and free-standing films represents a crucial step towards potentially using these coatings to prevent microbial attachment in high-touch applications.

MATERIALS AND METHODS

Materials and Chemicals. All compounds, unless otherwise noted, were used as received. Poly(4-styrenesulfonic acid, sodium salt) (PSS, AkzoNobel, VERSA TL130, 15 wt%, ca. 70,000 g/mol, N~340) was filtered using a 0.22 μm pore size filter (EMD Millipore) prior to use. Poly(diallyldimethylammonium chloride) (PDADMAC, Hyperfloc CP 626, 20 wt%, ca. 400,000 g/mol, N~2,470) was purchased from Hychem (Tampa, FL). Poly(2-methacryloyloxyethyl phosphorylcholine) was purchased from Sigma-Aldrich and purified by washing with anhydrous diethyl ether. M9 minimal salts (M9 media), D-(+)-glucose, Luria-Bertani broth (LB), carbenicillin (BioReagent grade), dopamine hydrochloride, and propidium iodide (PI) were purchased from Sigma-Aldrich. Tris hydrochloride, Tris base, potassium bromide (KBr, ACS grade), hydrogen chloride (HCl, ACS grade), sodium hydroxide (NaOH, ACS grade), acetone (ACS reagent), and square glass coverslips (22 mm × 22 mm) were purchased from Fisher Scientific (Hampton, NH). Barnstead Nanopure deionized (DI) water was obtained from a Milli-Q integral water purification system (resistivity of 18.2 MΩ cm, Millipore). The release layer LOR 5A (poly(dimethylglutarimide)) was purchased from Microchem (Westborough, MA), and silicon wafers (3 inch, Type P, 100 orientation) were purchased from University Wafer (Boston, MA).

RD6 developer (2.25-2.30% tetramethylammonium hydroxide in water) was purchased from Futurrex (Franklin, NJ).

Preparation of Complex Coacervates. Aqueous stock solutions of PSS and PDADMAC were prepared gravimetrically at a concentration of 0.5 M on a monomer basis and adjusted to pH 7.2 with a few drops of concentrated HCl or NaOH. A stock solution of 4 M KBr was also prepared gravimetrically. Liquid complex coacervates were prepared at a total volume of 10 mL with a final concentration of 0.1 M polymer, on a monomer basis, and a total KBr concentration of 1.6 M unless otherwise specified. PSS, KBr, and DI water were added into a 15 mL centrifuge tube (Fisher Scientific) followed by PDADMAC. The system was then vortexed for 30 sec and placed into a bath sonicator (Branson Ultrasonic Bath 2800, 40 kHz transducer) for 15 min to facilitate mixing and equilibration. The resulting mixture was then centrifuged at 5000 rpm for 10 min (Sorvall ST 16R Centrifuge, Thermo Fisher Scientific) to coalesce the dense, polymer-rich coacervate phase. The polymer-poor supernatant phase was removed from the coacervate phase using a transfer pipette.

Fabrication of Immobilized Coatings and Free-Standing PEC Films. Clean substrates (silicon wafers and glass coverslips) were prepared by rinsing with acetone, drying using nitrogen gas, and an oxygen plasma treatment (Harrick Plasma) for 1 min. Next, 2 mL of isolated coacervate phase was uniformly dispensed and spin-coated (G3P-8, Specialty Coating System) onto the cleaned substrates. Varying spin rates from 1000 rpm to 3000 rpm were evaluated using a 5 sec ramp and a 1 min hold time for all samples. The resulting PEC coating was immediately immersed into a 23 °C DI water bath (1 L) for 10 min to remove salt and to allow the film to solidify. After removing

the samples from the water bath, excess water was removed by blotting with a Kimwipe (Kimtech). This process produced PEC coatings that were immobilized on a substrate.

For free-standing films, a release layer of LOR 5A (poly(dimethylglutarimide)) was first spin-coated onto the cleaned substrate at 3000 rpm for 1 min, followed by heating at 190 °C for 3 min and 1 min of oxygen plasma treatment. After spin-coating the coacervate using the procedure previously described, samples were immersed in RD6 developer (2.25-2.30% tetramethylammonium hydroxide in water) for 5 hr to dissolve the LOR 5A layer, which released the film. The released PEC film was then rinsed using DI water.

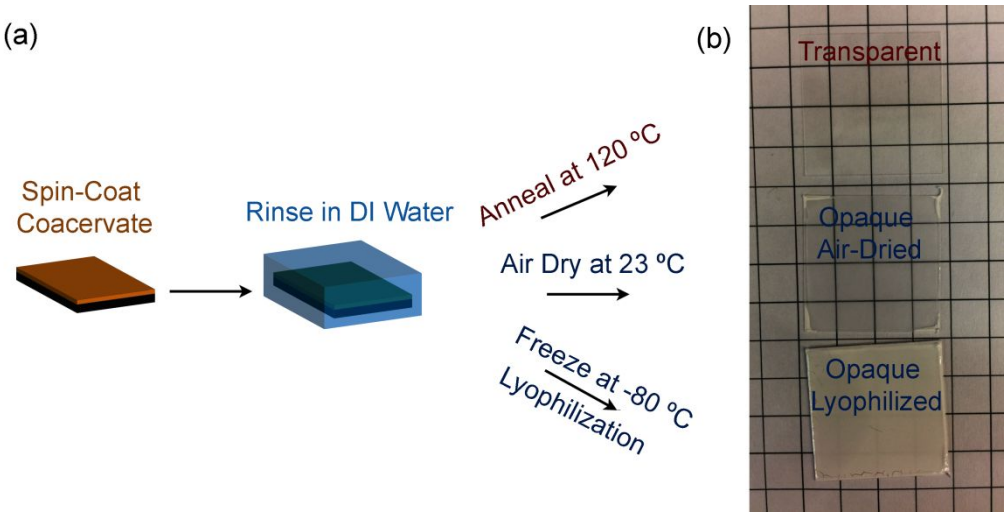

Figure 1. (a) General fabrication schematic and **(b)** photographs of transparent, opaque air-dried, and opaque lyophilized PEC films. For a schematic of the full process, see **Figure S1**.

Fabrication of Transparent and Opaque PEC Films. The transparency of immobilized and free-standing films was modulated post spin-coating. Transparent films were produced by annealing the water-saturated film at 120 °C on a hot plate (Fisher Scientific) for 1 min. Opaque films were obtained by either allowing the films to dry at 23 °C or by freezing the water-saturated film at -80 °C overnight, followed by lyophilization (FreeZone, Labconco) (**Figures 1** and **S1**).

PEC Film Characterization. PEC films used for characterization tests were prepared from coacervates made in 1.6 M KBr and spin-coated at 2000 rpm. The transparency of PEC films was measured by placing films immobilized on glass slides on top of a 96-well plate. The transmittance of the film was measured in triplicate using a Synergy plate reader (BioTek) from 310 - 750 nm wavelengths. Film thickness measurements were determined using a stylus profilometer (Dektak 3, Veeco/Sloan, Santa Barbara, CA) and a micrometer. Films attached to surfaces were first scratched using a razor blade to reveal the underlying substrate. Measurement scans were then run perpendicular to the scratches for a length of 2000 μm at a duration of 20 sec at 0.1 mm/s using 500 point resolution.[59] The thickness was determined to be the difference between the surface height and the lowest point of the scratch. Our profilometer data showed a clean substrate without roughness in the area of the scratch, confirming complete film removal. Film thicknesses were measured in triplicate. Free-standing films used for mechanical property characterization were measured using a Mitutoyo 293-330 digital micrometer by taking three measurements on each sample tested.

Small- and wide-angle X-ray scattering (SAXS/WAXS) was used to characterize the internal structure of the PEC films using a Ganesha SAXS-Lab with Cu Kα X-ray source (1.54 Å). Samples were prepared by folding one free-standing PEC film many times to achieve a total thickness of 0.5 - 1.6 mm. Film samples were placed into the center opening of a metal washer and fixed using Kapton tape before being mounted on the X-ray beam. Exposure times of 10 min and 3 min were used for SAXS and WAXS, respectively. Intensity data was normalized by the peak of WAXS region during analysis. Contact angle measurements were performed using 4 μL drops of DI water and glycerol using a home-built contact angle apparatus that was equipped with a Nikon D5100 digital camera with a 60-mm lens and 68-mm extension tube (Nikon, Melville,

NY).[60] At least 9 measurements were acquired on each type of film and the images were analyzed using *ImageJ 1.51j8* software (National Institutes of Health, Bethesda, MD).

Uniaxial mechanical testing was conducted using a Texture Analyzer (Texture Technologies) on free-standing PEC films (1 cm × 3 cm). Ultimate tensile stress was calculated by dividing the measured maximum force by the cross-sectional area of the film. The cross-sectional area was the product of the film width times thickness (based on micrometer measurements). The PEC films were mounted on two clips using a silicone rubber sheet (McMaster-Carr) as the mounting medium and stretched at an extension rate of ~3 mm/min until failure. Tests were conducted on 10 transparent films and 6 opaque films.

Evaluation of Antibacterial and Antifouling Activity of PEC Films. The Gram-negative microorganism, *Escherichia coli* K12 MG1655 *(E. coli*, DSMZ, Leibniz-Institut, Germany) containing a green fluorescent protein (GFP) plasmid was used in antibacterial and antifouling tests. *E. coli* (inoculated with 100 μg/mL carbenicillin) was cultured overnight in Luria-Bertani broth at 37 °C to a concentration of 10^8 cells/mL, washed twice, and resuspended in M9 media before their use in either antibacterial or antifouling experiments.

For antibacterial tests, PEC films and polymer zwitterion controls were placed in separate wells of 6-well polystyrene plates (Fisher Scientific), submerged in 5 mL of M9 media containing 10^8 *E. coli* cells, and incubated without shaking at 37 °C for 2 hr. Internal glass coverslips (cleaned by submerging in acetone at room temperature for 15 min followed by rinsing with autoclaved DI water three times, dried at ~100 °C for 1 hr, and treated with UV/ozone (UV/Ozone ProCleanerTM, Bioforce Nanosciences, Ames, IA) for 15 min) were run in parallel for each experiment. Cells were stained in the dark with PI (60 μM, excitation/emission at 535 nm/617 nm), allowed to

incubate for 15 min,[61] and rinsed gently with M9 media before acquiring 15 random images taken over 3 parallel replicates for 3 biological replicates using a Zeiss Microscope Axio Imager A2M (20x objective). GFP expressing *E. coli* were considered viable, while PI-stained *E. coli* were considered dead. *ImageJ 1.51j8* software was used to quantify the viable and dead cells and the percentage of viable bacteria was determined using Equation 1.

$$\text{Viable } E.\,coli\ (\%) = \frac{\text{Viable } E.\,coli}{\text{Viable } E.\,coli + \text{Dead } E.\,coli} \times 100 \quad \text{(Equation 1)}$$

Antifouling tests were conducted on PEC films and polymer zwitterion controls, which were prepared based on a previously published method.[9] Briefly, clean square glass coverslips (22 mm × 22 mm) were immersed in a solution of 10 mM Tris buffer (pH 8.5), poly(2-methacryloyloxyethyl phosphorylcholine) (polymer zwitterion, 2 mg/mL), and dopamine hydrochloride (2 mg/mL) for 6 hr at 23 °C. Excess polymer was removed via gentle rinsing with DI water, before the samples were air dried at 23 °C. Antifouling tests were conducted by placing PEC films and polymer zwitterion controls in separate wells of 6-well polystyrene plates and exposing them to 5 mL of *E. coli* (10^8 cells/mL of M9 media) without shaking for 24 hr at 37 °C. Samples were gently rinsed using M9 media and 15 randomly acquired images taken over 3 parallel replicates for 3 biological replicates were analyzed using *ImageJ* software to calculate the bacteria colony area coverage over the acquired 5,504,455 μm^2 area. Statistical significance was determined using a two-tailed, unpaired student *t*-test.

RESULTS AND DISCUSSION

Characteristics of PEC Films. Spin-coating was used to successfully fabricate uniform coatings from complex coacervates formed from salt (KBr) and two commercially-purchased, strong

polyelectrolytes, poly(4-styrenesulfonic acid, sodium salt) (PSS) and poly(diallyldimethylammonium chloride) (PDADMAC), see **Figures 1** and **S1.** Due to the hydrophilic nature of polyelectrolytes, substrates were first treated with oxygen plasma to facilitate good adhesion between the film and substrate and to avoid dewetting during the spin-coating process. This strategy allowed us to successfully prepare films on silicon wafers and glass slides in both the presence and absence of a polymeric release layer.

Freshly spin-coated films were transparent, however, they became opaque after being immersed in a water bath, which removes the salt (**Figure 1**). The amount of salt removed from the films was not directly quantified, but diffusion calculations based on results from Ghostine *et al*. suggest that rinsing of the films for a few seconds should be sufficient to remove nearly all of the salt.[62] However, the increased opacity of the films suggests the formation of a non-uniform structure, potentially clusters of ions and water that are large enough to scatter light. Films removed from the water bath remained opaque if they were dried under ambient conditions or if they were lyophilized, similar to the work by Costa *et al*.[45] Furthermore, once dried, the opacity of opaque films persisted after being immersed in water. Interestingly, films that were annealed at 120 °C after salt removal immediately created a highly transparent film, and they maintained transparency despite subsequent humidity treatment. Similar film transparency could also be obtained by exposing a dried opaque film to hot steam or boiling water. Overall, annealing the films caused them to be very stable and more transparent than processing the films using steam or boiling water. We hypothesize that this transformation from opaque to transparent is the result of temperature and water-facilitated rearrangement of the polymer chains that allows for the relaxation of sub-micron clusters of water and ions that would otherwise scatter light. The literature describes a decrease in the gas permeability of analogous PEC films after thermal annealing in humid

conditions.[63] Transmittance experiments demonstrated that annealed PEC films had a similar transparency to glass slides in the wavelength range of 310 – 750 nm, while air-dried films prepared using the same spin speed transmitted only ~65% of the incident light, and lyophilized films were opaque (**Figure S2**).

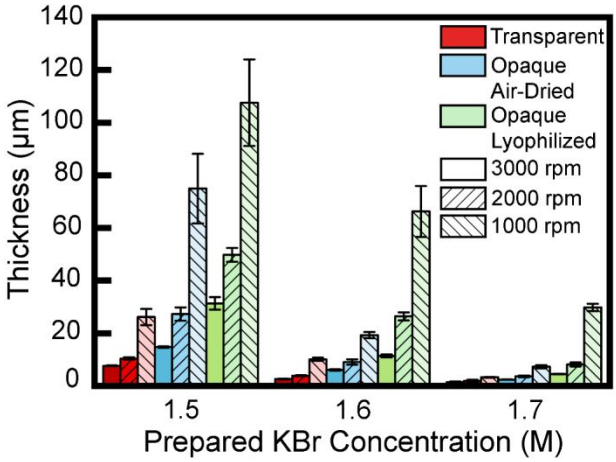

Figure 2. The thickness of immobilized transparent, opaque air-dried, and opaque lyophilized PEC films as a function of the as-prepared salt concentration and spin-coating speed. Error bars denote standard deviation.

PEC film thickness was investigated as a function of initial salt concentration, spin-coating speed, and post-treatment strategy (**Figure 2**). Film thickness decreased with increasing salt concentration and increasing spin speed, consistent with a report by Kelly and Schlenoff.[43] These results were expected because the viscosity of the PSS/PDADMAC coacervate used for spin-coating decreases with increasing salt concentration,[38,43,64,65] allowing for the formation of thinner films. Similarly, increasing the spin speed increases the centrifugal force, which subsequently thins the film. Comparing our results with those reported by Kelly and Schlenoff for the same polymer system,[43] our films were significantly thinner (*e.g.*, approximately 2.5 μm vs. 7.5 μm for samples prepared at 1.7 M KBr and 2000 rpm). The difference in thickness is not surprising because the

shorter polyelectrolytes used in our study lead to a coacervate solution that has a lower viscosity than the coacervate reported by Kelly and Schlenoff (*i.e.*, 0.92 Pa s vs. 1.42 Pa s).[64]

Post-processing also had the potential to influence film thickness. Lyophilized films were the thickest and potentially had a greater porosity, as suggested by their increased opacity, while transparent films were the thinnest. Specifically, at a salt concentration of 1.6 M and a spin rate of 2000 rpm, lyophilized films were roughly six times thicker than those prepared by thermal annealing and two times thicker than those prepared by air drying. Analysis via SAXS and WAXS suggest that the post-processing method did not significantly affect the molecular-level structure of the films (**Figure S3**). However, the scattering signal for the opaque films was consistently higher than the signal of the transparent films at low q, suggesting that differences in the structure may exist at larger length scales (*i.e.*, smaller q-values) than what was accessible in the measurement. This possibility of larger aggregates agrees with the observed differences in transparency and the potential for sub-micron scale clusters.

DI water and glycerol are two liquids that have different surface tensions and viscosities. Therefore, we conducted contact angle experiments using these two different liquids to determine the wettability of the transparent and opaque PEC films, **Figure 3**. To be considered hydrophilic, a material typically has a contact angle less than 90°; notably, hydrophilic surfaces have been reported to have strong antifouling properties, including an improved resistance to adhesion by bacteria.[5,6] Polymer zwitterion films with known hydrophilicity were used as controls.[9] Water contact angles for transparent, opaque air-dried, and opaque lyophilized PEC films were 33.9 ± 2.6°, 31.2 ± 2.7°, and 28.9 ± 4.2°, respectively, which are all statistically higher than the polymer zwitterion films (14.2 ± 2.7°). Similarly, the glycerol contact angles for transparent, opaque air-dried, and opaque lyophilized PEC films were 50.7 ± 4.2°, 48.4 ± 4.3°, and 40.1 ± 2.7°,

respectively, again, statistically greater than the glycerol contact angle of the polymer zwitterion films (32.8 ± 3.7°). While the polymer zwitterion control was more hydrophilic than the PEC films, the PEC films are still considered hydrophilic.

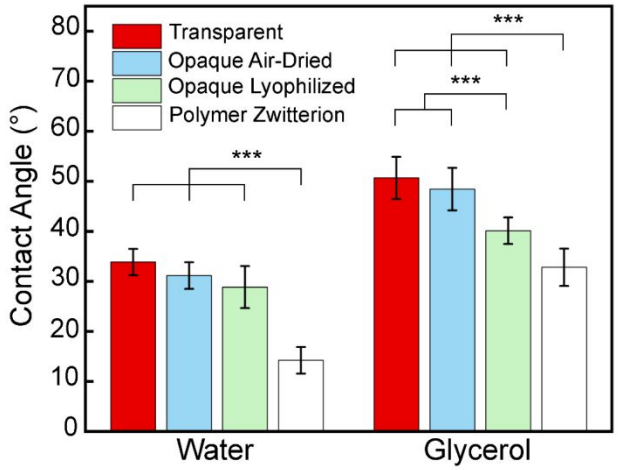

Figure 3. DI water and glycerol contact angle measurements of transparent and opaque PEC films, as well as polymer zwitterion controls. PEC films were prepared using PSS/PDADMAC with 1.6 M KBr and spin-coated at 2000 rpm. Three asterisks (***) denote 99.9% significance between samples. Error bars denote standard deviation.

PEC materials have long been considered intractable for processing. Due to the electrostatic interactions driving their self-assembly, PEC materials have excellent resistance against dissolution by organic solvents.[39] We have previously demonstrated this resistance for fiber mats that were electrospun using the same PEC system used in this work.[41] Additionally, the strong polyelectrolytes used in this study are resistant to variations in pH value. As a result, we expect that our films would show similar durability to the previously demonstrated PEC materials, including our fibers. Most interestingly, while high concentrations of salt have been shown to plasticize PEC materials, our thermally annealed PEC films were unaffected by immersion in a 4 M KBr solution, even after one month. This result suggests the possibility of using thermal treatment to further enhance the stability of a wide range of PEC-based materials.

In addition to the transparency, wetting, and physical stability of our films, mechanical properties are critical for enabling the use of high-performance coatings in real world settings. To this end, we performed uniaxial tensile tests on free-standing transparent and opaque PEC films. The transparent PEC films exhibited an ultimate tensile strength that was remarkably 4.2-fold greater than the opaque air-dried PEC films and stronger than other reported PEC films (**Figures 4** and **S4**). The average Young's modulus of the transparent films was found to be 29.07 ± 8.2 MPa, whereas a value of 6.01 ± 0.9 MPa was obtained for the opaque air-dried films. As evident from our reported standard deviations and **Figure S4**, which displays the stress-strain curves from which the mechanical properties were calculated, the transparent films exhibited more sample-to-sample variation than the opaque air-dried films. All free-standing PEC films exhibited a brittle fracture towards the middle of the films with a correspondingly low strain value of ~2%, previous reports also suggested that PECs have a low strain at break of ~5%.[43] In general, our data is consistent with other reports that demonstrate increased mechanical properties after annealing,[44,66,67] and we attribute the increase in ultimate tensile stress to an increase in the concentration of ionic bonds in the material, as well as a removal of stress-concentrating defects associated with the sub-micron clusters associated with the opacity of the untreated material.

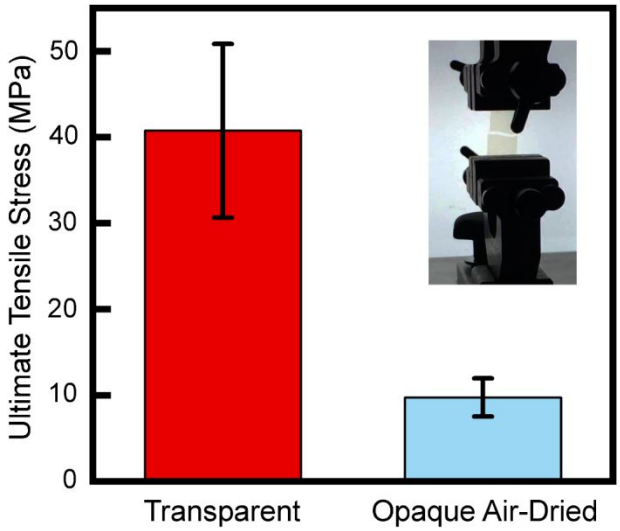

Figure 4. Ultimate tensile stress of transparent and opaque PEC films. Inset photo displays the experimental setup. PEC films were prepared using PSS/PDADMAC with 1.6 M KBr and spin-coated at 2000 rpm. Error bars denote standard deviation. Stress-strain curves acquired on the transparent and opaque PEC films are provided in **Figure S4**.

To determine if the PEC films inactivated microorganisms, we conducted a live/dead assay using *E. coli* (**Figure 5**). Transparent PEC films, polymer zwitterion control films, and glass had a negligible effect on *E. coli* viability, with statistically equivalent viability of at least 90%, indicating no killing. While cationic polymers, including the one we used to form our coacervate films, PDADMAC, have antibacterial properties,[61] the ion pairing of equimolar concentrations of PSS with PDADMAC eliminated these antibacterial properties. Our findings are consistent with experiments conducted on ultracentrifugated compact polyelectrolyte complexes formed from chitosan and alginate, which also demonstrated negligible killing of *Staphylococcus aureus*.[58] Charge-neutral polyelectrolyte complexes do not exhibit the antibacterial properties of their cationic polyelectrolyte components. Liquid complex coacervates have also been reported to be biocompatible with mammalian cells.[68,69]

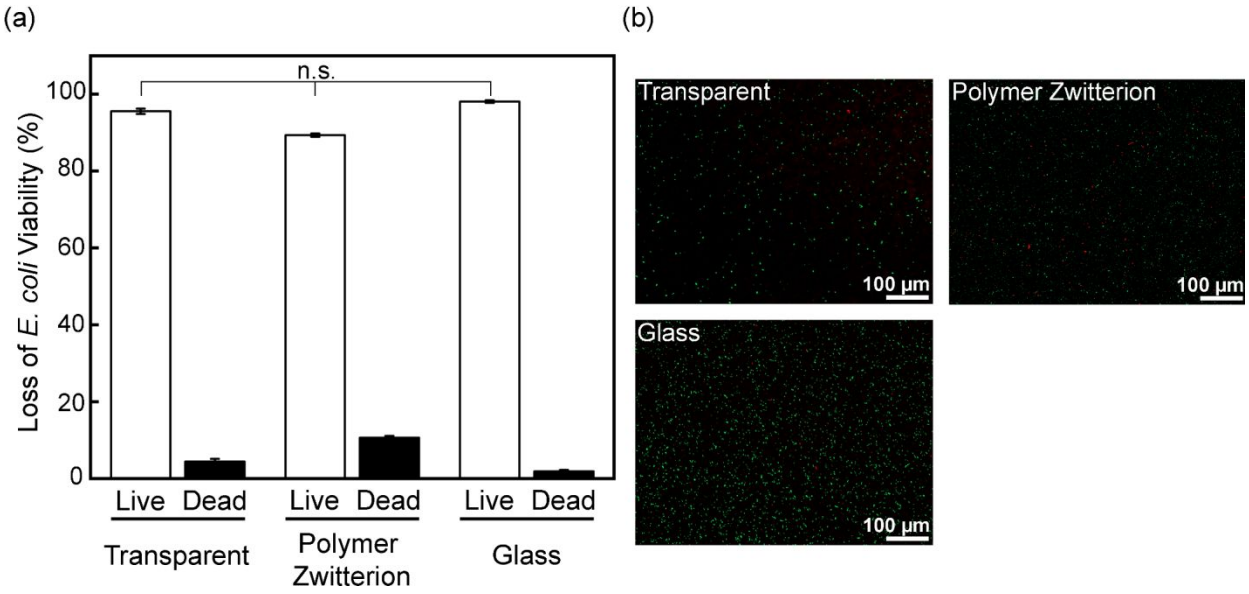

Figure 5. (a) *E. coli* viability and **(b)** representative micrographs of *E. coli* after a 2 hr incubation with transparent PEC films, as well as polymer zwitterion and glass controls. Errors bars denote standard error and n.s. indicates no statistical significance.

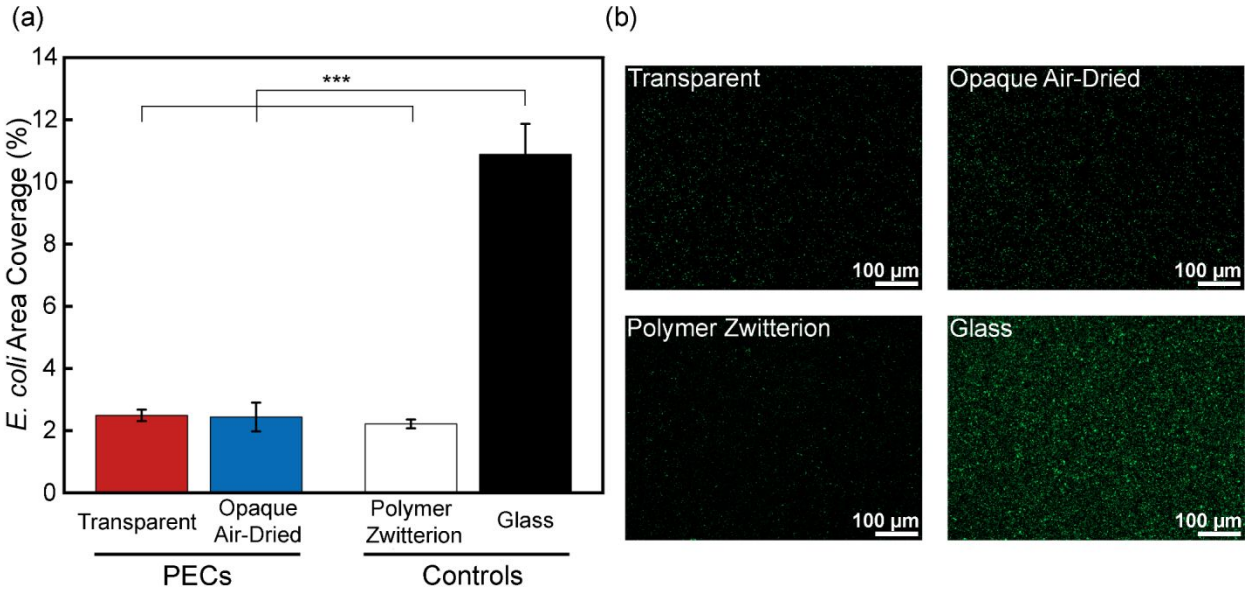

Figure 6. (a) Antifouling activity and **(b)** representative micrographs of transparent and opaque PEC films, as well as polymer zwitterion and glass controls after a 24 hr incubation with *E. coli*. Three asterisks (***) denote 99.9% significance between samples. Error bars denote standard error.

The antifouling properties (how many bacteria adhere) to the PEC films were assessed using *E. coli* cultured in minimal media, **Figure 6**. In comparison to control glass slides, PEC films

reduced the adhesion of *E. coli* by over 75%, from ~11% for glass to ~2.5% for transparent and air-dried PEC films. Furthermore, we observed a statistically equivalent performance between the PEC films and the polymer zwitterion coatings. While quantification was not provided for bacterial adhesion on ultracentrifuged compact PECs formed from chitosan and alginate, qualitative comparisons suggest comparable performance.[58] Our results demonstrate that PEC films are extremely antifouling to the microorganism *E. coli*, regardless of their transparency; and are equivalent to the polymer zwitterion films.

The hydrophilicity and strong microbial resistance properties of the PEC films are likely due to the proximity of positive and negative charges that bind PEC materials together. Sum frequency generation (SFG) spectroscopy measurements on zwitterionic and a 1:1 mixed charge polymer surface demonstrated strong levels of surface hydration, and thus antifouling character.[3,5–8] Furthermore, the use of polyelectrolyte complexation as a processing strategy allows for the formation of stable, water-insoluble films without the need for organic solvents. It should be noted that one limitation of our current PEC films is that they did not prevent the attachment of the protein, bovine serum albumin, **Figure S5**. While beyond the scope of this study, it is possible that by incorporating small concentrations of PEG or polymer zwitterions. nto the PEC films that their protein fouling resistance would be enhanced. The results from this study indicate that PEC films have the potential to offer an economic means of decreasing bacterial attachment.

CONCLUSION

We have established a straightforward method to fabricate robust, transparent, ultra-low bacterial-fouling PEC films via spin-coating of complex coacervates, followed by thermal annealing in a humid environment. The ability to create such resilient materials using water-only processing

allows for environmentally friendly processing and can facilitate the use of PEC-based coatings in a wide range of applications. Notably, the absence of any organic solvents or crosslinking agents allows for the safety and biocompatibility necessary for implementing antifouling coatings. This work paves the way for future exploration of novel PEC-based materials, including their use in biomedical applications as coatings for inanimate surfaces in hospitals and non-invasive biomedical equipment.

Supporting Information. Schematic of film preparation, as well as the transmittance, SAXS, WAXS, stress-strain curves, and bovine serum albumin adsorption to films is provided. The Supporting Information is available and free of charge http://pubs.acs.org.

ACKNOWLEDGEMENTS. We acknowledge the support of the National Science Foundation (NSF CMMI-1727660). I.S.K. acknowledges the support of the National Science Foundation NRT-SMLS program (DGE-1545399). M.H. was supported by National Research Service Award T32 GM008515 from the National Institutes of Health. We would also like to thank Dr. Todd Emrick, Xiangxi Meng, and Dr. Benjamin Yavitt for their helpful conversations.

REFERENCES

(1) Agodi, A.; Barchitta, M.; Cipresso, R.; Giaquinta, L.; Romeo, M. A.; Denaro, C. Pseudomonas Aeruginosa Carriage, Colonization, and Infection in ICU Patients. *Intensive Care Med.* **2007**, *33* (7), 1155–1161. https://doi.org/10.1007/s00134-007-0671-6.

(2) Kurtz, I. S.; Schiffman, J. D. Current and Emerging Approaches to Engineer Antibacterial and Antifouling Electrospun Nanofibers. *Materials* **2018**, *11* (7), 1059. https://doi.org/10.3390/ma11071059.

(3) Leng, C.; Huang, H.; Zhang, K.; Hung, H. C.; Xu, Y.; Li, Y.; Jiang, S.; Chen, Z. Effect of Surface Hydration on Antifouling Properties of Mixed Charged Polymers. *Langmuir* **2018**, *34* (22), 6538–6545. https://doi.org/10.1021/acs.langmuir.8b00768.

(4) Schlenoff, J. B. Zwitteration: Coating Surfaces with Zwitterionic Functionality to Reduce Nonspecific Adsorption. *Langmuir* **2014**, *30* (32), 9625–9636. https://doi.org/10.1021/la500057j.

(5) Hower, J. C.; Bernards, M. T.; Chen, S.; Tsao, H. K.; Sheng, Y. J.; Jiang, S. Hydration of "Nonfouling" Functional Groups. *J. Phys. Chem. B* **2009**, *113* (1), 197–201. https://doi.org/10.1021/jp8065713.

(6) White, A.; Jiang, S. Local and Bulk Hydration of Zwitterionic Glycine and Its Analogues through Molecular Simulations. *J. Phys. Chem. B* **2011**, *115* (4), 660–667. https://doi.org/10.1021/jp1067654.

(7) Evers, L. H.; Bhavsar, D.; Mailänder, P. The Biology of Burn Injury. *Exp. Dermatol.* **2010**, *19* (9), 777–783. https://doi.org/10.1111/j.1600-0625.2010.01105.x.

(8) Tegoulia, V. A.; Rao, W.; Kalambur, A. T.; Rabolt, J. F.; Cooper, S. L. Surface Properties, Fibrinogen Adsorption, and Cellular Interactions of a Novel Phosphorylcholine-Containing Self-Assembled Monolayer on Gold. *Langmuir* **2001**, *17* (14), 4396–4404. https://doi.org/10.1021/la001790t.

(9) Chang, C.-C.; Kolewe, K. W.; Li, Y.; Kosif, I.; Freeman, B. D.; Carter, K. R.; Schiffman, J. D.; Emrick, T. Underwater Superoleophobic Surfaces Prepared from Polymer Zwitterion/Dopamine Composite Coatings. *Adv. Mater. interfaces* **2016**, *3* (6), 1500521. https://doi.org/10.1002/admi.201500521.

(10) Banerjee, I.; Pangule, R. C.; Kane, R. S. Antifouling Coatings: Recent Developments in the Design of Surfaces That Prevent Fouling by Proteins, Bacteria, and Marine Organisms. *Adv. Mater.* **2011**, *23* (6), 690–718. https://doi.org/10.1002/adma.201001215.

(11) Hucknall, A.; Rangarajan, S.; Chilkoti, A. In Pursuit of Zero: Polymer Brushes That Resist the Adsorption of Proteins. *Adv. Mater.* **2009**, *21* (23), 2441–2446. https://doi.org/10.1002/adma.200900383.

(12) Mi, L.; Jiang, S. Integrated Antimicrobial and Nonfouling Zwitterionic Polymers. *Angew. Chemie - Int. Ed.* **2014**, *53* (7), 1746–1754. https://doi.org/10.1002/anie.201304060.

(13) Li, G.; Cheng, G.; Xue, H.; Chen, S.; Zhang, F.; Jiang, S. Ultra Low Fouling Zwitterionic Polymers with a Biomimetic Adhesive Group. *Biomaterials* **2008**, *29* (35), 4592–4597. https://doi.org/10.1016/j.biomaterials.2008.08.021.

(14) Keefe, A. J.; Jiang, S. Poly(Zwitterionic)Protein Conjugates Offer Increased Stability without Sacrificing Binding Affinity or Bioactivity. *Nat. Chem.* **2012**, *4* (1), 59–63. https://doi.org/10.1038/nchem.1213.

(15) Kyomoto, M.; Moro, T.; Takatori, Y.; Kawaguchi, H.; Nakamura, K.; Ishihara, K. Self-Initiated Surface Grafting with Poly(2-Methacryloyloxyethyl Phosphorylcholine) on Poly(Ether-Ether-Ketone). *Biomaterials* **2010**, *31* (6), 1017–1024. https://doi.org/10.1016/j.biomaterials.2009.10.055.

(16) Kuang, J.; Messersmith, P. B. Universal Surface-Initiated Polymerization of Antifouling Zwitterionic Brushes Using a Mussel-Mimetic Peptide Initiator. *Langmuir* **2012**, *28* (18), 7258–7266. https://doi.org/10.1021/la300738e.

(17) Zhang, Z.; Chao, T.; Chen, S.; Jiang, S. Superlow Fouling Sulfobetaine and Carboxybetaine Polymers on Glass Slides. *Langmuir* **2006**, *22* (24), 10072–10077. https://doi.org/10.1021/la062175d.

(18) Chang, Y.; Shih, Y. J.; Lai, C. J.; Kung, H. H.; Jiang, S. Blood-Inert Surfaces via Ion-Pair Anchoring of Zwitterionic Copolymer Brushes in Human Whole Blood. *Adv. Funct. Mater.* **2013**, *23* (9), 1100–1110. https://doi.org/10.1002/adfm.201201386.

(19) Futamura, K.; Matsuno, R.; Konno, T.; Takai, M.; Ishihara, K. Rapid Development of Hydrophilicity and Protein Adsorption Resistance by Polymer Surfaces Bearing Phosphorylcholine and Naphthalene Groups. *Langmuir* **2008**, *24* (18), 10340–10344. https://doi.org/10.1021/la801017h.

(20) Seo, J. H.; Matsuno, R.; Takai, M.; Ishihara, K. Cell Adhesion on Phase-Separated Surface of Block Copolymer Composed of Poly(2-Methacryloyloxyethyl Phosphorylcholine) and Poly(Dimethylsiloxane). *Biomaterials* **2009**, *30* (29), 5330–5340. https://doi.org/10.1016/j.biomaterials.2009.06.031.

(21) Ueda, T.; Oshida, H.; Kurita, K.; Ishihara, K.; Nakabayashi, N. Preparation of 2-Methacryloyloxyethyl Phosphorylcholine Copolymers with Alkyl Methacrylates and Their Blood Compatibility. *Polym. J.* **1992**, *24* (11), 1259–1269. https://doi.org/10.1295/polymj.24.1259.

(22) D'souza, A. A.; Shegokar, R. Polyethylene Glycol (PEG): A Versatile Polymer for Pharmaceutical Applications. *Expert Opin. Drug Deliv.* **2016**, *13* (9), 1257–1275. https://doi.org/10.1080/17425247.2016.1182485.

(23) Abuchowski, A.; McCoy, J. R.; Palczuk, N. C.; van Es, T.; Davis, F. F. Effect of Covalent Attachment of Polyethylene Glycol on Immunogenicity and Circulating Life of Bovine Liver Catalase. *J. Biol. Chem.* **1977**, *252* (11), 3582–3586.

(24) Knop, K.; Hoogenboom, R.; Fischer, D.; Schubert, U. S. Poly(Ethylene Glycol) in Drug Delivery: Pros and Cons as Well as Potential Alternatives. *Angew. Chemie - Int. Ed.* **2010**, *49* (36), 6288–6308. https://doi.org/10.1002/anie.200902672.

(25) Kolate, A.; Baradia, D.; Patil, S.; Vhora, I.; Kore, G.; Misra, A. PEG - A Versatile Conjugating Ligand for Drugs and Drug Delivery Systems. *J. Control. Release* **2014**, *192* (28), 67–81. https://doi.org/10.1016/j.jconrel.2014.06.046.

(26) Ulbricht, J.; Jordan, R.; Luxenhofer, R. On the Biodegradability of Polyethylene Glycol, Polypeptoids and Poly(2-Oxazoline)S. *Biomaterials* **2014**, *35* (17), 4848–4861. https://doi.org/10.1016/j.biomaterials.2014.02.029.

(27) McGary, C. W. Degradation of Poly(Ethylene Oxide). *J. Polym. Sci.* **1960**, *46* (147), 51–

57. https://doi.org/10.1002/pol.1960.1204614705.

(28) Han, S.; Kim, C.; Kwon, D. Thermal/Oxidative Degradation and Stabilization of Polyethylene Glycol. *Polymer* **1997**, *38* (2), 317–323. https://doi.org/10.1016/S0032-3861(97)88175-X.

(29) Branch, D. W.; Wheeler, B. C.; Brewer, G. J.; Leckband, D. E. Long-Term Stability of Grafted Polyethylene Glycol Surfaces for Use with Microstamped Substrates in Neuronal Cell Culture. *Biomaterials* **2001**, *22* (10), 1035–1047. https://doi.org/10.1016/S0142-9612(00)00343-4.

(30) Pidhatika, B.; Rodenstein, M.; Chen, Y.; Rakhmatullina, E.; Mühlebach, A.; Acikgöz, C.; Textor, M.; Konradi, R. Comparative Stability Studies of Poly(2-Methyl-2-Oxazoline) and Poly(Ethylene Glycol) Brush Coatings. *Biointerphases* **2012**, *7* (1), 1. https://doi.org/10.1007/s13758-011-0001-y.

(31) Yang, Q.; Lai, S. K. Anti-PEG Immunity: Emergence, Characteristics, and Unaddressed Questions. *Wiley Interdiscip. Rev. Nanomedicine Nanobiotechnology* **2015**, *7* (5), 655–677. https://doi.org/10.1002/wnan.1339.

(32) Zhang, P.; Sun, F.; Liu, S.; Jiang, S. Anti-PEG Antibodies in the Clinic: Current Issues and beyond PEGylation. *J. Control. Release* **2016**, *244*, 184–193. https://doi.org/10.1016/j.jconrel.2016.06.040.

(33) Yang, Q.; Jacobs, T. M.; McCallen, J. D.; Moore, D. T.; Huckaby, J. T.; Edelstein, J. N.; Lai, S. K. Analysis of Pre-Existing IgG and IgM Antibodies against Polyethylene Glycol (PEG) in the General Population. *Anal. Chem.* **2016**, *88* (23), 11804–11812. https://doi.org/10.1021/acs.analchem.6b03437.

(34) Blocher, W. C.; Perry, S. L. Complex Coacervate-Based Materials for Biomedicine. *Wiley Interdiscip. Rev. Nanomedicine Nanobiotechnology* **2017**, *9* (4), e1442. https://doi.org/10.1002/wnan.1442.

(35) Sing, C. E. Development of the Modern Theory of Polymeric Complex Coacervation. *Adv. Colloid Interface Sci.* **2017**, *239*, 2–16. https://doi.org/10.1016/j.cis.2016.04.004.

(36) Priftis, D.; Laugel, N.; Tirrell, M. Thermodynamic Characterization of Polypeptide Complex Coacervation. *Langmuir* **2012**, *28* (45), 15947–15957. https://doi.org/10.1021/la302729r.

(37) Perry, S. L.; Li, Y.; Priftis, D.; Leon, L.; Tirrell, M. The Effect of Salt on the Complex Coacervation of Vinyl Polyelectrolytes. *Polymers* **2014**, *6* (6), 1756–1772. https://doi.org/10.3390/polym6061756.

(38) Wang, Q.; Schlenoff, J. B. The Polyelectrolyte Complex/Coacervate Continuum. *Macromolecules* **2014**, *47* (9), 3108–3116. https://doi.org/10.1021/ma500500q.

(39) Michaels, A. S. Polyelectrolyte Complexes. *J. Macromol. Sci. Part A - Chem.* **1965**, *57*

(10), 32–40. https://doi.org/10.1080/10601326908053794.

(40) Kalantar, T. H.; Tucker, C. J.; Zalusky, A. S.; Boomgaard, T. A.; Wilson, B. E.; Ladika, M.; Jordan, S. L.; Li, W. K.; Zhang, X.; Goh, C. G. High Throughput Workflow for Coacervate Formation and Characterization in Shampoo Systems. *J. Cosmet. Sci.* **2007**, *58* (4), 375–383.

(41) Meng, X.; Perry, S. L.; Schiffman, J. D. Complex Coacervation: Chemically Stable Fibers Electrospun from Aqueous Polyelectrolyte Solutions. *ACS Macro Lett.* **2017**, *6* (5), 505–511. https://doi.org/10.1021/acsmacrolett.7b00173.

(42) Meng, X.; Schiffman, J. D.; Perry, S. L. Electrospinning Cargo-Containing Polyelectrolyte Complex Fibers: Correlating Molecular Interactions to Complex Coacervate Phase Behavior and Fiber Formation. *Macromolecules* **2018**, *51* (21), 8821–8832. https://doi.org/10.1021/acs.macromol.8b01709.

(43) Kelly, K. D.; Schlenoff, J. B. Spin-Coated Polyelectrolyte Coacervate Films. *ACS Appl. Mater. Interfaces* **2015**, *7* (25), 13980–13986. https://doi.org/10.1021/acsami.5b02988.

(44) Shamoun, R. F.; Reisch, A.; Schlenoff, J. B. Extruded Saloplastic Polyelectrolyte Complexes. *Adv. Funct. Mater.* **2012**, *22* (9), 1923–1931. https://doi.org/10.1002/adfm.201102787.

(45) Costa, R. R.; Costa, A. M. S.; Caridade, S. G.; Mano, J. F. Compact Saloplastic Membranes of Natural Polysaccharides for Soft Tissue Engineering. *Chem. Mater.* **2015**, *27* (21), 7490–7502. https://doi.org/10.1021/acs.chemmater.5b03648.

(46) Gai, M.; Frueh, J.; Kudryavtseva, V. L.; Mao, R.; Kiryukhin, M. V.; Sukhorukov, G. B. Patterned Microstructure Fabrication: Polyelectrolyte Complexes vs Polyelectrolyte Multilayers. *Sci. Rep.* **2016**, *6*, 37000. https://doi.org/10.1038/srep37000.

(47) Hariri, H. H.; Schlenoff, J. B. Saloplastic Macroporous Polyelectrolyte Complexes: Cartilage Mimics. *Macromolecules* **2010**, *43* (20), 8656–8663. https://doi.org/10.1021/ma1012978.

(48) Porcel, C. H.; Schlenoff, J. B. Compact Polyelectrolyte Complexes: "Saloplastic" Candidates for Biomaterials. *Biomacromolecules* **2009**, *10* (11), 2968–2975. https://doi.org/10.1021/bm900373c.

(49) Wang, Q.; Schlenoff, J. B. Tough Strained Fibers of a Polyelectrolyte Complex: Pretensioned Polymers. *RSC Adv.* **2014**, *4* (87), 46675–46679. https://doi.org/10.1039/c4ra08733j.

(50) Liu, Q.; Li, Q.; Xu, S.; Zheng, Q.; Cao, X. Preparation and Properties of 3D Printed Alginate-Chitosan Polyion Complex Hydrogels for Tissue Engineering. *Polymers* **2018**, *10* (6), 664. https://doi.org/10.3390/polym10060664.

(51) Zhu, F.; Cheng, L.; Yin, J.; Wu, Z. L.; Qian, J.; Fu, J.; Zheng, Q. 3D Printing of

Ultratough Polyion Complex Hydrogels. *ACS Appl. Mater. Interfaces* **2016**, *8* (45), 31304–31310. https://doi.org/10.1021/acsami.6b09881.

(52) Diamanti, E.; Muzzio, N.; Gregurec, D.; Irigoyen, J.; Pasquale, M.; Azzaroni, O.; Brinkmann, M.; Moya, S. E. Impact of Thermal Annealing on Wettability and Antifouling Characteristics of Alginate Poly-L-Lysine Polyelectrolyte Multilayer Films. *Colloids Surfaces B Biointerfaces* **2016**, *145*, 328–337. https://doi.org/10.1016/j.colsurfb.2016.05.013.

(53) Kolasińska, M.; Warszyński, P. The Effect of Nature of Polyions and Treatment after Deposition on Wetting Characteristics of Polyelectrolyte Multilayers. *Appl. Surf. Sci.* **2005**, *252* (3), 759–765. https://doi.org/10.1016/j.apsusc.2005.02.060.

(54) Elzbieciak, M.; Kolasinska, M.; Warszynski, P. Characteristics of Polyelectrolyte Multilayers: The Effect of Polyion Charge on Thickness and Wetting Properties. *Colloids Surfaces A Physicochem. Eng. Asp.* **2008**, *321* (1–3), 258–261. https://doi.org/10.1016/j.colsurfa.2008.01.036.

(55) Francesko, A.; Ivanova, K.; Hoyo, J.; Pérez-Rafael, S.; Petkova, P.; Fernandes, M. M.; Heinze, T.; Mendoza, E.; Tzanov, T. Bottom-up Layer-by-Layer Assembling of Antibacterial Freestanding Nanobiocomposite Films. *Biomacromolecules* **2018**, *19* (9), 3628–3636. https://doi.org/10.1021/acs.biomac.8b00626.

(56) Tripathi, B. P.; Dubey, N. C.; Stamm, M. Functional Polyelectrolyte Multilayer Membranes for Water Purification Applications. *J. Hazard. Mater.* **2013**, *252–253*, 401–412. https://doi.org/10.1016/j.jhazmat.2013.02.052.

(57) Zhu, X.; Jańczewski, D.; Lee, S. S. C.; Teo, S. L. M.; Vancso, G. J. Cross-Linked Polyelectrolyte Multilayers for Marine Antifouling Applications. *ACS Appl. Mater. Interfaces* **2013**, *5* (13), 5961–5968. https://doi.org/10.1021/am4015549.

(58) Phoeung, T.; Spanedda, M. V.; Roger, E.; Heurtault, B.; Fournel, S.; Reisch, A.; Mutschler, A.; Perrin-Schmitt, F.; Hemmerlé, J.; Colin, D.; Rawiso, F.; Boulmedais, F.; Schaaf, P.; Lavalle, P.; Frisch, B. Alginate/Chitosan Compact Polyelectrolyte Complexes: A Cell and Bacterial Repellent Material. *Chem. Mater.* **2017**, *29* (24), 10418–10425. https://doi.org/10.1021/acs.chemmater.7b03863.

(59) Rieger, K. A.; Eagan, N. M.; Schiffman, J. D. Encapsulation of Cinnamaldehyde into Nanostructured Chitosan Films. *J. Appl. Polym. Sci.* **2015**, *132* (13). https://doi.org/10.1002/app.41739.

(60) Ishino, C.; Okumura, K.; Quéré, D. Wetting Transitions on Rough Surfaces. *Europhys. Lett.* **2004**, *68* (3), 419–425. https://doi.org/10.1209/epl/i2004-10206-6.

(61) Rieger, K. A.; Porter, M.; Schiffman, J. D. Polyelectrolyte-Functionalized Nanofiber Mats Control the Collection and Inactivation of Escherichia Coli. *Materials* **2016**, *9* (4), 297. https://doi.org/10.3390/ma9040297.

(62) Ghostine, R. A.; Markarian, M. Z.; Schlenoff, J. B. Asymmetric Growth in Polyelectrolyte Multilayers. *J. Am. Chem. Soc.* **2013**, *135* (20), 7636–7646. https://doi.org/10.1021/ja401318m.

(63) Haile, M.; Henderson, R.; Grunlan, J. C.; Sarwar, O.; Smith, R. Polyelectrolyte Coacervates Deposited as High Gas Barrier Thin Films. *Macromol. Rapid Commun.* **2017**, *38* (1), 1600594. https://doi.org/10.1002/marc.201600594.

(64) Liu, Y.; Momani, B.; Winter, H. H.; Perry, S. L. Rheological Characterization of Liquid-to-Solid Transitions in Bulk Polyelectrolyte Complexes. *Soft Matter* **2017**, *13* (40), 7332–7340. https://doi.org/10.1039/c7sm01285c.

(65) Spruijt, E.; Cohen Stuart, M. A.; Van Der Gucht, J. Linear Viscoelasticity of Polyelectrolyte Complex Coacervates. *Macromolecules* **2013**, *46* (4), 1633–1641. https://doi.org/10.1021/ma301730n.

(66) Wang, X. S.; Ji, Y. L.; Zheng, P. Y.; An, Q. F.; Zhao, Q.; Lee, K. R.; Qian, J. W.; Gao, C. J. Engineering Novel Polyelectrolyte Complex Membranes with Improved Mechanical Properties and Separation Performance. *J. Mater. Chem. A* **2015**, *3* (14), 7296–7303. https://doi.org/10.1039/c4ta06477a.

(67) Cai, N.; Han, C.; Luo, X.; Liu, S.; Yu, F. Rapidly and Effectively Improving the Mechanical Properties of Polyelectrolyte Complex Nanofibers through Microwave Treatment. *Adv. Eng. Mater.* **2017**, *19* (1), 1600483. https://doi.org/10.1002/adem.201600483.

(68) Black, K. A.; Priftis, D.; Perry, S. L.; Yip, J.; Byun, W. Y.; Tirrell, M. Protein Encapsulation via Polypeptide Complex Coacervation. *ACS Macro Lett.* **2014**, *3* (10), 1088–1091. https://doi.org/10.1021/mz500529v.

(69) Giannotti, M. I.; Abasolo, I.; Oliva, M.; Andrade, F.; García-Aranda, N.; Melgarejo, M.; Pulido, D.; Corchero, J. L.; Fernández, Y.; … Schwartz, S. Highly Versatile Polyelectrolyte Complexes for Improving the Enzyme Replacement Therapy of Lysosomal Storage Disorders. *ACS Appl. Mater. Interfaces* **2016**, *8* (39), 25741–25752. https://doi.org/10.1021/acsami.6b08356.

(70) Elder, R. M.; Emrick, T.; Jayaraman, A. Understanding the Effect of Polylysine Architecture on DNA Binding Using Molecular Dynamics Simulations. *Biomacromolecules* **2011**, *12* (11), 3870–3879. https://doi.org/10.1021/bm201113y.

TOC